

A numerical investigation of the behaviour of the minimum ignition energy for turbulent droplet-laden mixtures

V.S. Papapostolou, G. Ozel-Erol, C. Turquand d'Auzay, N. Chakraborty,
School of Engineering, Newcastle University, Newcastle upon Tyne, UK

1 Introduction

The phenomenon by which the initiation and subsequent combustion of a flammable mixture occurs due to externally imposed means, (i.e. electrical or laser induced spark, plasma jet or heated surface) is known as forced ignition. Forced ignition is of fundamental interest in turbulent reacting flows, but also due to its practical importance for industrial applications (e.g. Spark Ignition engines, industrial gas turbines, high altitude relight etc.), it has been studied extensively across a wide range of configurations. Significant efforts have been directed towards the investigation of the forced ignition of droplet laden mixtures, both experimentally and computationally, and key findings from existing literature have been summarised by Mastorakos [1]. However limited effort has been directed towards the fundamental understanding of the nature of the variation of the minimum ignition energy (MIE, the threshold energy required to ignite a flammable mixture) in regards to varying droplet diameters, overall (liquid and gaseous phase) equivalence ratios and turbulence intensities, and thus the present study aims to address this gap in the existing literature. In the present analysis, three dimensional Direct Numerical Simulations (DNS) of localised forced ignition for n-heptane droplets with different initial turbulence intensities, droplet diameters and overall equivalence ratios under decaying homogeneous isotropic turbulence have been carried out to evaluate the minimum energy required to (i) obtain at least a successful ignition and to (ii) obtain a successful ignition followed by a self-sustained combustion once the ignitor has been switched off. The main objective of this work is to understand and illustrate the effects of initial turbulence intensities, droplet diameters and overall equivalence ratios have on the behaviour of MIE for forced ignition of droplet laden mixtures.

2 Mathematical Background & Numerical Implementation

A modified single step Arrhenius type irreversible chemical reaction is chosen for the current analysis, to keep the computational cost of the study within reasonable limits. Three-dimensional DNS simulations with detailed chemistry would be exorbitantly expensive for the current parametric analysis, consisting of three different turbulence intensities, droplet diameters and overall equivalence ratio. The following single-step irreversible reaction has thus been considered, $\text{Fuel} + s \cdot \text{Oxidiser} \rightarrow (1 + s)\text{Products}$, where s is the mass of

oxygen consumed per unit mass of fuel consumption. The chemical mechanism was implemented following the previous work of Tarrazo et al. [2], where the activation energy, E_{ac} , and the heat of combustion have been taken to be functions of the gaseous equivalence ratio, ϕ_g , which provides a realistic equivalence ratio dependence for the unstrained laminar burning velocity $S_{L(\phi_g=1)}$ in hydrocarbon-air flames. The Lewis number ($Le_i = \alpha_i/D_i$ where α_i is the thermal diffusivity and D_i is the species diffusivity of the i^{th} species) of all species was taken to be unity, while all species in the gaseous phase are ideal gases, and thus for compressible flow DNS, as is the case here, the ideal gas law applies. Standard values were taken for the ratio of specific heats ($\gamma = C_p^g/C_v^g = 1.4$, where C_p^g and C_v^g are the gaseous specific heats at constant pressure and volume, respectively) and Prandtl number ($Pr = \mu C_p^g/\lambda = 0.7$, where μ is the dynamic viscosity and λ is the thermal conductivity of the gaseous phase). Each individual droplet is tracked in a Lagrangian sense, whilst the compressible Navier-Stokes equations are solved in the Eulerian frame for the carrier gaseous phase. The evolution of the droplet related quantities such as the position, \vec{x}_d , velocity, \vec{u}_d , diameter a_d and temperature T_d are expressed following the work of Reveillon and Vervisch [3]. The coupling between Lagrangian and Eulerian phases is obtained from the additional source terms in the gaseous phase transport equations [3,4]:

$$\frac{\partial \rho \psi}{\partial t} + \frac{\partial \rho u_j \psi}{\partial x_j} = \frac{\partial}{\partial x_j} (\Gamma_\psi \frac{\partial \psi_1}{\partial x_j}) + \dot{w}_\psi + \dot{S}_g + \dot{S}_\psi \quad (1)$$

where $\psi = \{1, u_i, e, Y_F, Y_O\}$ and $\psi_1 = \{1, u_i, \hat{T}, Y_F, Y_O\}$ for the conservation equations of mass, momentum, energy, and fuel and oxidiser mass fraction, respectively, and \hat{T} is the dimensional temperature. For $\psi = \{1, u_i, Y_F, Y_O\}$, $\Gamma_\psi = \rho\nu/\sigma_\psi$, however for $\psi = e$, $\Gamma_\psi = \lambda$ and u_i represents velocity in the i^{th} direction. The \dot{w}_ψ term arises due to the chemical reaction rate, \dot{S}_g is an appropriate source/sink term in the gaseous phase, \dot{S}_ψ is the appropriate source term due to droplet evaporation which is tri-linearly interpolated from the droplets sub grid position, \vec{x}_d , to the eight surrounding nodes, whilst ν represents kinematic viscosity and σ_ψ refers to an appropriate Schimdt number corresponding to ψ . An additional source term, ($q''' = A_{sp} \exp(-r^2/2R_{sp}^2)$ with r being the distance from the ignitor centre and R_{sp} representing the characteristic width of energy deposition) is added to the energy conservation equation, which follows a Gaussian distribution in the radial direction from the ignition centre, as used in previous studies [5]. The constant A_{sp} is determined by a volume integration which leads to the total ignition power \dot{Q} given by:

$$\dot{Q} = \int_V q''' dV = a_{sp} \rho_0 C_p \tau T_0 \left(\frac{4}{3}\pi \delta_z^3\right) \left[\frac{\mathcal{H}(t) - \mathcal{H}(t - t_{sp})}{t_{sp}}\right] \quad (2)$$

where a_{sp} is a parameter determining the total energy deposited by the ignitor, $\tau = (T_{ad(\phi_g=1)} - T_0)/T_0$ is the heat release parameter (where $T_{ad(\phi_g=1)}$ and T_0 are the adiabatic flame temperature of the stoichiometric mixture and unburned gas temperature respectively), δ_z is the Zel'dovich flame thickness ($\delta_z = D_0/S_{L(\phi_g=1)}$, where D_0 is the reactants mass diffusivity and $S_{L(\phi_g=1)}$ is the unstrained laminar burning velocity of the stoichiometric mixture) and $\mathcal{H}(t)$, and $\mathcal{H}(t - t_{sp})$ are Heaviside functions which ensure that the ignitor is only active until $t = t_{sp}$. The energy deposition duration t_{sp} , is expressed as $t_{sp} = b_{sp} t_f$, where $t_f = \delta_z/S_{L(\phi_g=1)}$ is a characteristic timescale and the energy deposition parameter b_{sp} is given a value of $b_{sp} = 0.2$ in the present study, which falls within its optimal range as outlined by [1]. In the present study, the energy deposition duration (b_{sp}) and width (R_{sp}) are kept constant, whilst the ignition power, a_{sp} is modified until the MIE is found for both successful ignition and propagation. It is vital to distinguish between the two, as a successful ignition does not ensure subsequent self sustained flame propagation [5]. A successful ignition refers to a situation where the maximum temperature surpasses the adiabatic flame temperature at any point in time. If the maximum temperature does not reach the adiabatic flame temperature, it is referred to as a misfire. A successful self-sustained propagation is obtained

when the flame kernel burns without the aid of the ignitor after a successful ignition. It is determined by evaluating the temporal evolution of the burned gas volume, and if its temporal derivative is positive at $t = 10t_{sp}$, a successful self sustained propagation is obtained, otherwise it is considered to be quenched. The simulations have been carried out using the three-dimensional compressible DNS code SENGAs [4,5] in a domain of size $51\delta_z \times 51\delta_z \times 51\delta_z$ or $9.6l_t \times 9.6l_t \times 9.6l_t$. The domain is discretized by a Cartesian grid of $264 \times 264 \times 264$ cells of uniform size Δx , which ensures 10 grid points across the thermal flame thickness $\delta_{th} = [T_{ad(\phi_g=1)} - T_0] / \max(|\nabla \hat{T}|_L)$. It also ensures $\eta_k > \Delta x$, where η_k is the Kolmogorov length scale. The boundaries of the domain are considered to be partially non-reflecting. The spatial differentiation and time advancements have been carried out using high order finite difference and explicit Runge-Kutta schemes respectively. The flame-turbulence interaction takes place under decaying isotropic homogeneous turbulence. A well-known pseudo-spectral method [6] is used to initialise the turbulent velocity fluctuation by an incompressible, homogeneous isotropic field with prescribed values of root-mean-square (rms) values (u') and integral length scale (l_t). The flammable mixture consists of n-heptane droplets uniformly dispersed in air and the overall equivalence ratio (ϕ_{ov}) is determined by the number of droplets initially present in the domain. Three different droplet diameters a_d are investigated ($a_d/\delta_{th} = 0.03, 0.04, 0.05$), across three different global equivalence ratios ($\phi_{ov} = 0.8, 1.0, 1.2$). All three droplet diameters and global equivalence ratios are investigated across three different initial turbulence intensities ($u'/S_{L(\phi_g=1)} = 0.0, 4.0, 8.0$). The droplets' initial temperature (T_0) is taken to be 300K, which yields a heat release parameter of $\tau = 6.54$, and all cases investigated are under atmospheric pressure conditions. Care was taken to ensure that the droplet diameter remains smaller than the Kolmogorov length scale for all cases investigated, and the ratio of initial droplet diameter to the Kolmogorov length scales is $a_d/\eta_k = 0.22, 0.29, 0.36$ for $a_d/\delta_{th} = 0.03, 0.04, 0.05$, respectively, for the highest initial turbulence intensity investigated. The ratio a_d/η_k is comparable to several previous analyses by other authors [1,3,4], and thus the assumption of sub-grid evaporation is not expected to significantly affect the ignition phenomenon and subsequent flame-droplet interaction.

3 Results & Discussion

The non-dimensional temperature ($T = (\hat{T} - T_0) / (T_{ad,\phi_g=1} - T_0)$) iso-surfaces at different time instants are shown in Fig. 1 for different cases and for each case the normalised energy (Γ) deposited by the spark corresponds to its respective normalised MIE, Γ_{MIE}^p . The quantity Γ is defined as $\Gamma = IE / MIE_l^{\phi_g=1.0}$, where IE is the energy deposited by the ignitor and $MIE_l^{\phi_g=1.0}$ is the MIE for self-sustained flame propagation of a laminar n-heptane premixed stoichiometric mixture. In the present analysis, the laminar MIE is given by $MIE_l^{\phi_g=1.0} / [\rho_0 C_p \tau T_0 (\frac{4}{3} \pi \delta_z^3)] = 4.8$. The superscripts i and p are used to refer to ignition and propagation respectively. For ease of reference and brevity each case will be referred to in the following manner: U00, U04, U08 refer to $u'/S_{L(\phi_g=1)} = 0, 4, 8$ respectively; D03, D04, D05 refer to $a_d/\delta_{th} = 0.03, 0.04, 0.05$ respectively, and F08, F10, F12 refer to $\phi_{ov} = 0.8, 1.0, 1.2$ respectively. Figure 1 illustrates the effects of turbulence intensity, droplet size and overall equivalence ratio on Γ_{MIE}^i and Γ_{MIE}^p . For U00D05F12 the kernel retains its spherical structure as expected for laminar conditions [5], but droplets induce flame wrinkling, and this ‘‘dimpling’’ effect has been observed in both experimental and computational studies [1,4]. For the turbulent cases shown here, the kernel becomes increasingly wrinkled and deformed as time advances, along with the aforementioned dimpling effect due to the droplets, but the effects of turbulence dominate over the droplet induced wrinkling as shown in previous studies [4]. The difference in size of the isosurfaces at $t = 2t_{sp}$ between U08D03F08 and the other two cases presented in Fig. 1 is indicative that the energy requirement to obtain a successful propagation differs significantly as the initial turbulence

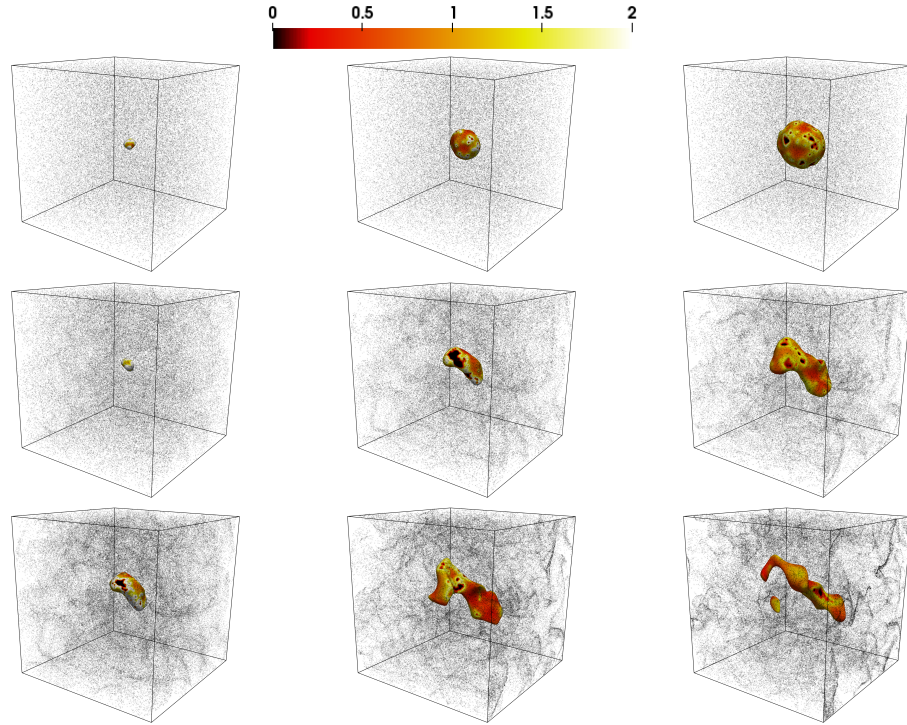


Figure 1: Isosurfaces of $T = 0.7$ at times $t = 2, 5, 8t_{sp}$ (left to right) for cases U00D05F12, U04D04F10 and U08D03F08 (top to bottom), with $\Gamma = \Gamma_{MIE}^p$ for each case respectively, coloured by reaction rate.

intensity increases, but is also affected to a lesser, but still significant extent by the initial droplet diameter and overall equivalence ratio. This variation in the MIE required to obtain a successful ignition and a self sustained propagation is illustrated by Fig. 2, where the effects of $u'/S_{L(\phi_g=1)}$, a_d/δ_{th} and ϕ_{ov} on Γ_{MIE}^i and Γ_{MIE}^p can be seen for all cases. Observing the variation of Γ_{MIE}^i from Fig. 2, as turbulence increases so does the MIE requirement, and the effects of turbulence dominate over the effects induced by the change in droplet diameter and ϕ_{ov} . As shown by previous studies [5], both Γ_{MIE}^i and Γ_{MIE}^p increase with increasing turbulence intensity. The MIE slowly increases for moderate values of $u'/S_{L(\phi_g=1)}$ but a more rapid increase in Γ_{MIE}^i and Γ_{MIE}^p is observed for large values of $u'/S_{L(\phi_g=1)}$, as shown in Fig. 2 for Γ_{MIE}^p for cases U08*. Thus, it is instructive to examine two sets of cases, the laminar cases for Γ_{MIE}^i , and the U08* cases for Γ_{MIE}^p , to observe the effects of droplet diameter and overall equivalence ratio, giving rise to two key observations. Firstly, as the initial overall equivalence ratio increases, $\Gamma_{MIE}^{i/p}$ decreases and secondly,

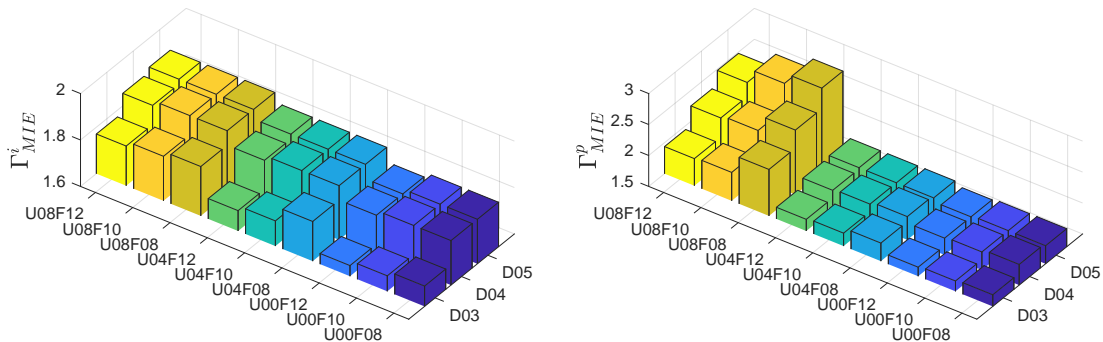


Figure 2: Normalised MIE for successful ignition (Γ_{MIE}^i , left) and propagation (Γ_{MIE}^p , right), across all cases.

as the droplet diameter increases, $\Gamma_{MIE}^{i/p}$ increases. The effects of ϕ_{ov} on $\Gamma_{MIE}^{i/p}$ are consistent across all cases investigated, and can be most clearly seen for the laminar cases with D03. However, droplet diameter has a stronger influence on the variation of $\Gamma_{MIE}^{i/p}$ than the overall equivalence ratio does within the parameter range considered here, and this can be most easily seen from the difference in energy requirements as droplet diameter increases (i.e. the difference of Γ_{MIE}^p from U08F08D03 to U08F08D04 to U08F08D05) as opposed to when the overall equivalence ratio decreases and $\Gamma_{MIE}^{i/p}$ increases (i.e. the difference of Γ_{MIE}^i from U00F12D03 to U00F10D03 to U00F08D03). The cases chosen here to illustrate these effects, are the ones where the effects are the most visible, however the relationships described hold across all cases investigated. To understand the physical effects which have been observed, it is necessary to understand that igniting droplet-laden mixtures requires more energy than igniting a homogeneous mixture, as in the case of droplets extra energy is required to evaporate the fuel, which subsequently allows for ignition. The MIE variation shown in Fig. 2 can be explained in terms of the probability density functions (PDFs) of gaseous equivalence ratio (ϕ_g) which are shown in Fig. 3 for the time instant $t = 5t_{sp}$. Observing Figs. 2 and 3 in conjunction, it can be understood why both Γ_{MIE}^i and Γ_{MIE}^p drastically increases from D03 to D04, but minimally increases from D04 to D05. As initial droplet diameter increases, so too does the energy require-

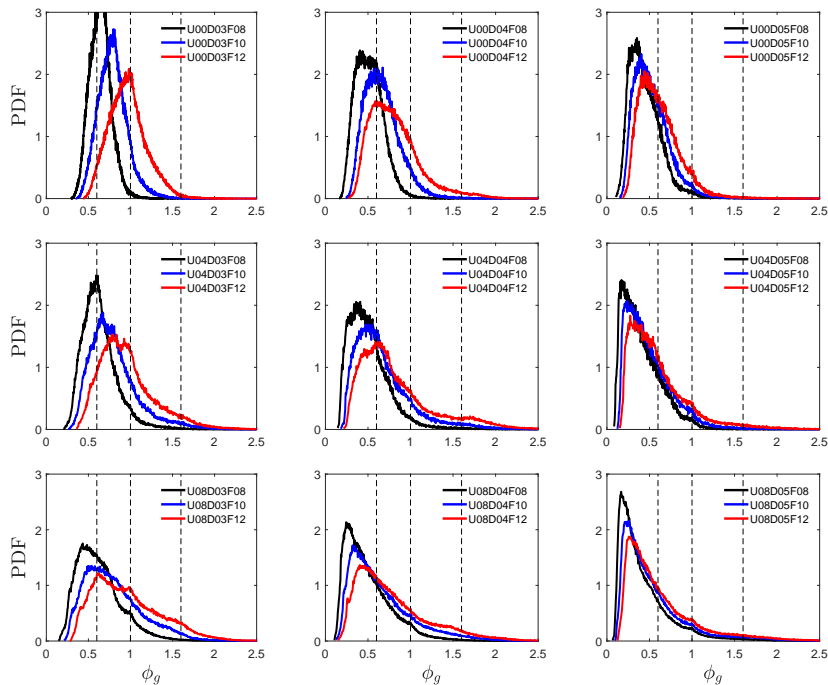


Figure 3: PDF of gaseous equivalence ratio (ϕ_g) for all cases, with $\Gamma = \Gamma_{MIE}^p$ at $t = 5t_{sp}$. The lean and rich flammability limits and stoichiometric mixture composition are shown by the vertical dashed black lines.

ment to preheat and evaporate the droplets [1], and to subsequently create a gaseous flammable mixture ($0.6 < \phi_g < 1.6$). As the droplet diameter increases, the probability of finding flammable gaseous mixtures decreases, as the peak value of the PDFs shift outside of the lean flammability limits, as can be seen in Fig. 3. Across all cases, the probability of finding gaseous mixtures within the flammability limits is significantly higher for D03, but for D04 and D05 the PDFs of ϕ_g peak at, or below the lean flammability limit. Additionally, the PDFs for D04 and D05 exhibit very similar behaviour (peaking outside the lean flammability limit), but the PDFs of D03 indicate a significantly higher likelihood of encountering flammable mixtures, which in turn leads to a smaller MIE requirement. It must be mentioned that ϕ_{ov} also has a smaller but

significant influence. As ϕ_{ov} increases, so does the probability of finding ϕ_g close to unity, thus allowing for easier propagation, which in turn corresponds to smaller Γ_{MIE}^i and Γ_{MIE}^p requirements, as observed in Fig. 2. The effects of ϕ_{ov} are consistent for all cases, but these effects weaken with increasing a_d/δ_{th} and $u'/S_{L(\phi_g=1)}$, as illustrated by the cases with D05, where the difference in ϕ_{ov} , minimally affects the profile and peaks of the PDFs of ϕ_g . Lastly as the initial turbulence intensity increases, the peaks of the PDFs of ϕ_g slightly shift towards leaner conditions, but these effects are minimal when compared to the effects induced by the change in initial droplet diameter and ϕ_{ov} .

4 Conclusions

The minimum ignition energy (MIE) for uniformly dispersed n-heptane droplet-laden mixtures in homogeneous isotropic decaying turbulence has been numerically evaluated for three different initial turbulence intensities, droplet diameters and overall equivalence ratios. The findings of the present study indicate that the size and number (global equivalence ratio) of droplets affect MIE in a complicated manner. Two key conclusions can be drawn from the present study. A smaller initial droplet diameter or a higher initial global equivalence ratio, reduces the MIE requirement and is beneficial towards successful ignition and subsequent self sustained propagation. The effects of increasing initial turbulence intensity have also been analysed and the MIE has been found to increase with increasing u' but a significant increase of the MIE was observed for large turbulence intensities, in accordance with previous MIE studies [5]. Additionally, it was shown that the MIE required for droplet laden mixtures, is higher than the relevant MIE required for a corresponding homogeneous mixture, due to the extra energy required to evaporate the droplets. The current analysis, excludes the effects of complex transport and low-temperature kinetics or gas ionisation effects on the ignition process and their influence on the MIE. However, the qualitative nature of the results is not expected to be affected if detailed chemistry were to be used. Further investigation of these effects with detailed chemistry and transport will form the basis of future investigations.

5 Acknowledgements

The financial support of British Council, EPSRC, and National Education Ministry of Turkish government and computational support of Rocket, Cirrus and ARCHER are gratefully acknowledged.

References

- [1] Mastorakos E. (2017). Forced ignition of turbulent spray flames. *Proc. Combust. Inst.* 36: 2367.
- [2] Tarrazo E. et al. (2006) A simple one-step chemistry model for partially premixed hydrocarbon combustion. *Combust. Flame* 147: 32.
- [3] Reveillon J. and Vervisch L (2000) Spray vaporization in non-premixed turbulent combustion modelling: A single droplet model. *Combust. Flame* 121: 75.
- [4] Ozel-Erol G. et al. (2018). A direct numerical simulation analysis of spherically expanding turbulent flames in fuel droplet-mists for an overall equivalence ratio of unity. *Phys. Fluids*. 30: 086104.
- [5] Turquand d'Auzay C. et al. (2019). On the minimum ignition energy and its transition in the localised forced ignition of turbulent homogeneous mixtures. *Combust. Flame*. 201: 104.
- [6] Rogallo R.S. (1981). Numerical experiments in homogeneous turbulence. Technical Report.